LBNL-39119
UC-405
Preprint

ERNEST ORLANDO LAWRENCE
BERKELEY NATIONAL LABORATORY

Consolidation of Common Parameters from Multiple Fits in Dynamic PET Data Analysis

R.H. Huesman and P.G. Coxson
Life Sciences Division

June 1996
Submitted to
IEEE Transactions on Medical Imaging

Consolidation of Common Parameters from Multiple Fits in Dynamic PET Data Analysis *

R.H. Huesman and P.G. Coxson
Center for Functional Imaging
E. O. Lawrence Berkeley National Laboratory
University of California

June 28, 1996

Abstract

In dynamic PET data analysis, regions of interest are analyzed by fitting a parametric model to the time-activity curve acquired after a radio-labeled tracer has been introduced into the patient's bloodstream. This procedure can be carried out for multiple regions of interest and/or multiple injections of the same or a different radiopharmaceutical. The approach presented here takes advantage of prior knowledge that some of the parameters of those multiple fits are the same. Reduction of the total number of parameters to be estimated results in smaller statistical uncertainty for all parameter estimates, especially those common to multiple fits.

Introduction

In dynamic positron emission tomography (PET) data analysis, regions of interest (ROIs) are analyzed by fitting a compartmental model to the time-activity curve acquired after a radio-labeled tracer has been introduced into the patient's blood[1]. The model we use for this purpose is:

$$y(t,\boldsymbol{p}) = f_v\, u(t-t_0) + (1-f_v)\int_{-\infty}^{t} h(\{k\},t-\tau)\, u(\tau-t_0)\, d\tau \ , \qquad (1)$$

*This work was supported in part by the National Heart, Lung and Blood Institute of the U.S. Department of Health and Human Services under Grants HL47675 and HL25840, and in part by the Director, Office of Energy Research, Office of Health and Environmental Research, Medical Applications and Biophysical Research Division of the U.S. Department of Energy under Contract DE-AC03-76SF00098.

where $y(t, \boldsymbol{p})$ is the time activity curve for the region of interest, u(t) is the time activity curve for the blood, f_v is the fraction of the region of interest which consists of blood, $\{k\}$ are the model parameters representing the transfer rate of tracer from one compartment to another, t_0 is the time offset between tissue and blood measurements, $h(\{k\}, t)$ is the impulse response function for the compartmental model, and $\boldsymbol{p}$ is the vector of parameters to be fit, $\boldsymbol{p} = (f_v, t_0, \{k\})^T$.

This fitting procedure can be carried out for multiple ROIs and/or multiple injections. The present work takes advantage of *a priori* knowledge that some of the parameters of these multiple fits are the same. For example, the time-delay t_0 between arrival of blood at the blood sampling site and arrival at an ROI can be expected to be nearly equal for different ROIs in the brain[2]. Also, the fractional blood volume f_v of an ROI can be expected to remain constant for certain multiple injection studies. Reduction of the total number of parameters to be estimated results in smaller statistical uncertainty for all parameter estimates, especially those common to multiple fits.

Ideally one would perform a grand fit for all of the time-activity curves which have any common parameters by minimizing the combined weighted sum of squared residuals. This is equivalent to maximum likelihood estimation, since the elements of the time-activity curve are samples taken from normally distributed random variables. In this way the common parameters are naturally constrained to have the same value in the models for different time-activity curves. We are often in the situation where the results of the separate fits are available, and we would like to be able to predict the results of the grand fit from the results of the separate fits. Here we investigate a method to approximate the results of the grand fit which is referred to here as the Grand Taylor Fit (GTF). It is based on Taylor polynomial approximations to the individual criteria which have been optimized in the separate fits. This approach results in simple formulas, amenable to hand calculation, for the estimation of parameters and their covariances. In particular, the common parameters are estimated as a weighted average of the results from the separate fits, and other parameter estimates are adjusted based on their correlations with the common parameters.

Studies involving a common blood fraction (f_v) illustrate the power and simplicity of this approach, and an example with common arrival times (t_0) shows some of the difficulties.

Formulation of the Grand Taylor Fit

Dynamic PET measurement data consists of accumulated emission counts y_j representing the integral of $y(t, \boldsymbol{p})$ over the time interval (t_{j-1}, t_j). Measurements y_j^i from the i^{th} data set are assumed to be normally distributed about the integral of $y(t, \boldsymbol{p}^i)$ with variances $\sigma^2(y_j^i)$. These variances are estimated by straightforward application of the ROI evaluation procedure given in [3].

Under these conditions, the criterion to be minimized to fit the parameter vector $\boldsymbol{p}$ to the i^{th} data set is the weighted sum of squared residuals of the form:

$$S_i = \sum_j \frac{\left[y_j^i - \int_{t_{j-1}}^{t_j} y(t, \boldsymbol{p}^i)\, dt\right]^2}{\sigma^2(y_j^i)} , \tag{2}$$

The maximum likelihood estimator of the parameter vector $\boldsymbol{p}$ for the i^{th} data set is denoted by $\hat{\boldsymbol{p}}^i$. The criterion can be approximated by the first two terms of a Taylor expansion of the criterion about its minimum:

$$S_i \approx S_{io} + (\boldsymbol{p}^i - \hat{\boldsymbol{p}}^i)^T (\Phi^i)^{-1} (\boldsymbol{p}^i - \hat{\boldsymbol{p}}^i) , \tag{3}$$

where S_{io} is the minimum value of the criterion, $\hat{\boldsymbol{p}}^i$ is the value of the parameter vector at the minimum, and Φ^i is our estimate of the covariance matrix of the single fit parameter estimate $\hat{\boldsymbol{p}}^i$. $(\Phi^i)^{-1}$ is obtained by calculating numerical second derivatives of S_i at the minimum. In order to facilitate incorporation of the *a priori* knowledge that some of the parameters represent the same quantity in all the fits, we separate the parameter vector, $\boldsymbol{p}^i$, into two components: $\boldsymbol{p}_a^i$ which is different for each i and $\boldsymbol{p}_b$ which is common to all fits:

$$\boldsymbol{p}^i = \begin{pmatrix} \boldsymbol{p}_a^i \\ \boldsymbol{p}_b \end{pmatrix} . \tag{4}$$

The criterion for the grand fit is the sum of the N individual criteria,

$$S_G = \sum_{i=1}^{N} S_i . \tag{5}$$

The solution to the grand fit, $\boldsymbol{p}_a^{Gi}$ and $\boldsymbol{p}_b^G$, are found by setting the derivatives of S_G with respect to $\boldsymbol{p}_a^i$ and $\boldsymbol{p}_b$ equal to zero. Using the Taylor expansions in equation (3) to approximate the individual criteria, we obtain explicit formulas for GTF approximations $\hat{\boldsymbol{p}}^G$ to the grand fit parameter estimates $\boldsymbol{p}^G$:

$$\hat{\boldsymbol{p}}_b^G = \left(\sum_{i=1}^{N} (\Phi_{bb}^i)^{-1}\right)^{-1} \sum_{i=1}^{N} (\Phi_{bb}^i)^{-1} \hat{\boldsymbol{p}}_b^i , \tag{6}$$

$$\hat{\boldsymbol{p}}_a^{Gi} = \hat{\boldsymbol{p}}_a^i + \Phi_{ab}^i (\Phi_{bb}^i)^{-1} (\hat{\boldsymbol{p}}_b^G - \hat{\boldsymbol{p}}_b^i) , \tag{7}$$

where we have used the following decomposition of Φ^i:

$$\Phi^i = \begin{pmatrix} \Phi_{aa}^i & \Phi_{ab}^i \\ \Phi_{ba}^i & \Phi_{bb}^i \end{pmatrix} . \tag{8}$$

Derivation of equations (6) and (7) is given in the appendix. They give us a prescription to estimate the outcome of the grand fit using only the results of the individual fits. Also derived in

the appendix are the following expressions for the diagonal blocks of Φ, the covariance matrix of the solution to the grand fit, as expressed in terms of the single fit covariance matrices:

$$\Phi(\hat{\boldsymbol{p}}_b^G, \hat{\boldsymbol{p}}_b^G) = \left(\sum_{k=1}^{N} (\Phi_{bb}^k)^{-1} \right)^{-1} . \tag{9}$$

$$\Phi(\hat{\boldsymbol{p}}_a^{Gi}, \hat{\boldsymbol{p}}_a^{Gi}) = \Phi_{aa}^i - \Phi_{ab}^i \left[(\Phi_{bb}^i)^{-1} - (\Phi_{bb}^i)^{-1} \Phi(\hat{\boldsymbol{p}}_b^G, \hat{\boldsymbol{p}}_b^G) (\Phi_{bb}^i)^{-1} \right] \Phi_{ba}^i , \tag{10}$$

Equation (6) shows that the new estimate of the common parameter vector is the weighted average of the results of the individual fits. Equation (9) shows that the variance of the new estimates of the common parameters is expected to be reduced by at most a factor of N, the number of fits. The maximum reduction is achieved when all of the Φ_{bb}^k are equal. The values of the remaining parameters are then changed to reflect their correlation with the common parameter, as illustrated by equation (7). Equation (10) shows that the variance of these parameters is also reduced. Both the parameter values and the variances determined from the Taylor approximations are biased estimates of the grand fit parameters and variances. The bias is zero if all of the individual Taylor series are second order. In our first example, the biases are small and in the second they are relatively large.

Example 1: Multiple Injections With a Common Region

For each of several ^{82}Rb injections in a single anesthetized dog, a sequence of PET measurements of the ^{82}Rb activity in a region of the myocardium and, simultaneously ($t_0 = 0$), the activity in the blood pool in the left ventricular cavity were taken over a period of 4-6 minutes[4, 5, 6, 7, 8]. These data were used to determine parameters k_{21} (uptake), k_{12} (washout), and f_v (vascular fraction) for the myocardial region, to fit the model

$$y(t, \boldsymbol{p}) = f_v \, u(t) + (1 - f_v) \int_{-\infty}^{t} k_{21} \, e^{-k_{12}(t-\tau)} \, u(\tau) \, d\tau \ . \tag{11}$$

Different injections were used to examine the change in k_{21} and k_{12} under a variety of physiologic conditions. We assume for the purpose of this analysis that the vascular fraction is unaffected by these conditions and should be the same in all fits. Table 1 shows the parameters estimated in five independent studies.

Plots in Figure 1 illustrate how the individual criterion values and the grand criterion value are affected by the choice of f_v. Each circle in the five plots on the left in Figure 1 is the minimum criterion value for that injection, conditioned on the value of f_v. The solid line is the quadratic function which has the same minimum and curvature at the minimum as the criterion curve. In the upper right panel of Figure 1, the grand criterion is shown with open circles, each representing

the sum of the minimum criterion values for the five injections. The best f_v is defined to be the vascular fraction which minimizes this curve, $f_v^G = 0.166$. Our estimate of the best common f_v is $\hat{f}_v^G = 0.166$, which minimizes the sum of the five quadratic functions — the solid line in that panel. Note that in this case it is indistinguishable from f_v^G and the quadratic curve provides a good approximation to the grand criterion.

Table 2 contains two sets of estimates: 1) the grand fit parameters estimates, and 2) the GTF approximations as calculated from equations (6) and (7) above:

$$\hat{f}_v^G = \frac{\sum \hat{f}_v^i / \sigma^2(f_v^i)}{\sum 1/\sigma^2(f_v^i)} , \tag{12}$$

$$\hat{k}_{21}^{Gi} = \hat{k}_{21}^i + \frac{\sigma(k_{21}^i)\,\rho(k_{21}^i, f_v^i)\,(\hat{f}_v^G - \hat{f}_v^i)}{\sigma(f_v^i)} , \tag{13}$$

$$\hat{k}_{12}^{Gi} = \hat{k}_{12}^i + \frac{\sigma(k_{12}^i)\,\rho(k_{12}^i, f_v^i)\,(\hat{f}_v^G - \hat{f}_v^i)}{\sigma(f_v^i)} . \tag{14}$$

The grand fit estimate of k_{21} and its approximation for first injection are shown graphically in the lower right panel of Figure 1. Each circle represents the best fit of k_{21} with f_v given by the abscissa, if all parameters except f_v are fit. Therefore the ordinate of the circle at $f_v = f_v^G$ is the grand fit estimate. The Taylor approximation to the grand fit estimate is given by the ordinate of the straight line at $f_v = \hat{f}_v^G$. The straight line is tangent to the locus of circles at $f_v = \hat{f}_v^1$.

Example 2: Multiple Regions with a Common Time Delay

For a single injection of ^{18}FDG in a human subject, a time series of PET measurements were taken in several regions of a single slice of the subject's brain[9, 10, 11]. The purpose of the study was to examine differences in glucose metabolism in different regions of the brain. Glucose metabolism is modeled using the blood activity curve and three kinetic rate parameters: k_{21}, k_{12}, and k_{32}. As in the rubidium example, tissue and blood data were combined to obtain estimates of the kinetic parameters. In this case our model is given by

$$y(t, \boldsymbol{p}) = f_v\, u(t - t_0) + (1 - f_v) \int_{-\infty}^{t} \frac{k_{21}}{k_{12} + k_{32}} \left[k_{12}\, e^{-(k_{12}+k_{32})(t-\tau)} + k_{32} \right] u(\tau - t_0)\, d\tau . \tag{15}$$

The blood data were collected at a remote location, since there was no measurable pool of blood in the transverse section of the brain in which the tissue regions were analyzed. Consequently, the time delay between the site of blood measurement (usually an artery in the arm) and the brain slice of interest must be estimated. This additional parameter, t_0, is assumed to be the same for all regions of the brain. Table 3 shows the parameters estimated in six independent studies.

Plots in Figure 2 illustrate how the individual criteria are affected by the choice of t_0. Each circle in the six regional plots in Figure 2 is the minimum criterion value for that region, conditioned on the value of t_0. The solid line is the quadratic function which has the same minimum and curvature at the minimum as the criterion curve. The grand criterion is shown in the tall plot with open circles, each representing the sum of the minimum criterion values for the six regions. The best t_0 is defined to be the time delay which minimizes this curve, $t_0^G = -12.8$. Our estimate of t_0^G is $\hat{t}_0^G = -13.1$, which minimizes the sum of the six quadratic functions — the solid line in the graph. In this example, $\hat{t}_0^G$ is noticeably different from t_0^G. The quadratic curves are relatively poor representations of the separate fits, so it is not surprising that the grand Taylor fits based on these quadratic functions produce biased estimates.

Table 4 gives the results of the grand fit with the parameter t_0 fit in common and lists the parameters obtained by the approximation method. In this example, the approximations to the grand fit are noticeably biased.

Conclusion

We have derived simple formulas based on Taylor approximations to multiple separate criteria for approximating parameters which would minimize the grand criterion, under an assumption that some parameters are common. The utility of this approach has been demonstrated in an example for which the Taylor approximation is appropriate. A second example demonstrated the difficulties of this approach for a case in which the common parameter (time delay) enters the optimization problem in a complicated way.

The approach developed in this paper was first presented at the 1990 IEEE Nuclear Science Symposium [12].

Acknowledgments

We would to thank Hector William Colon Rosa for assistance with data analysis. This work was supported in part by the National Heart, Lung and Blood Institute of the U.S. Department of Health and Human Services under Grants HL47675 and HL25840, and in part by the Director, Office of Energy Research, Office of Health and Environmental Research, Medical Applications and Biophysical Research Division of the U.S. Department of Energy under Contract DE-AC03-76SF00098.

Appendix

We rewrite equation 3, the Taylor expansion of the criterion for the i^{th} fit about its minimum as:

$$S_i = S_{io} + (\boldsymbol{p}^i - \hat{\boldsymbol{p}}^i)^T M^i (\boldsymbol{p}^i - \hat{\boldsymbol{p}}^i) \tag{16}$$

where S_{io} is the minimum value of the criterion, $\hat{\boldsymbol{p}}^i$ is the value of the parameter vector at the minimum, and M^i is the symmetric matrix whose inverse, Φ^i, is the covariance matrix of the single fit parameter estimate $\hat{\boldsymbol{p}}^i$. In order to facilitate incorporation of the *a priori* knowledge that some of the parameters represent the same quantity in all the fits, we separate the parameter vector, $\boldsymbol{p}^i$, into two components: $\boldsymbol{p}_a^i$ which is different for each i and $\boldsymbol{p}_b$ which is common to all fits:

$$\boldsymbol{p}^i = \begin{pmatrix} \boldsymbol{p}_a^i \\ \boldsymbol{p}_b \end{pmatrix} \tag{17}$$

so that equation (16) can be rewritten as

$$S_i = S_{io} + (\boldsymbol{p}_a^i - \hat{\boldsymbol{p}}_a^i)^T M_{aa}^i (\boldsymbol{p}_a^i - \hat{\boldsymbol{p}}_a^i) + 2(\boldsymbol{p}_b - \hat{\boldsymbol{p}}_b^i)^T M_{ba}^i (\boldsymbol{p}_a^i - \hat{\boldsymbol{p}}_a^i) + (\boldsymbol{p}_b - \hat{\boldsymbol{p}}_b^i)^T M_{bb}^i (\boldsymbol{p}_b - \hat{\boldsymbol{p}}_b^i) \tag{18}$$

where M^i, has the decomposition:

$$M^i = \begin{pmatrix} M_{aa}^i & M_{ab}^i \\ M_{ba}^i & M_{bb}^i \end{pmatrix} \tag{19}$$

The criterion for the grand fit is then written as the sum of the N individual criteria.

$$S_G = \sum_{i=1}^{N} S_i \tag{20}$$

$$= \sum_{i=1}^{N} S_{io} + \sum_{i=1}^{N} (\boldsymbol{p}_a^i - \hat{\boldsymbol{p}}_a^i)^T M_{aa}^i (\boldsymbol{p}_a^i - \hat{\boldsymbol{p}}_a^i) + 2\sum_{i=1}^{N} (\boldsymbol{p}_b - \hat{\boldsymbol{p}}_b^i)^T M_{ba}^i (\boldsymbol{p}_a^i - \hat{\boldsymbol{p}}_a^i) + \sum_{i=1}^{N} (\boldsymbol{p}_b - \hat{\boldsymbol{p}}_b^i)^T M_{bb}^i (\boldsymbol{p}_b - \hat{\boldsymbol{p}}_b^i) \tag{21}$$

The solution to the grand fit, $\hat{\boldsymbol{p}}_a^{Gi}$ and $\hat{\boldsymbol{p}}_b^G$, are found by setting the derivatives of S_G with respect to $\boldsymbol{p}_a^i$ and $\boldsymbol{p}_b$ equal to zero:

$$2M_{aa}^i (\hat{\boldsymbol{p}}_a^{Gi} - \hat{\boldsymbol{p}}_a^i) + 2M_{ab}^i (\hat{\boldsymbol{p}}_b^G - \hat{\boldsymbol{p}}_b^i) = 0 \tag{22}$$

$$2\sum_{i=1}^{N} M_{ba}^i (\hat{\boldsymbol{p}}_a^{Gi} - \hat{\boldsymbol{p}}_a^i) + 2\sum_{i=1}^{N} M_{bb}^i (\hat{\boldsymbol{p}}_b^G - \hat{\boldsymbol{p}}_b^i) = 0 \tag{23}$$

These are simplified using relations easily derived from expansion of the identity $M^i \Phi^i = I$:

$$M_{bb}^i - M_{ba}^i (M_{aa}^i)^{-1} M_{ab}^i = (\Phi_{bb}^i)^{-1} \tag{24}$$

$$(M^i_{aa})^{-1} M^i_{ab} = -\Phi^i_{ab} (\Phi^i_{bb})^{-1} \tag{25}$$

where Φ^i, has the decomposition:

$$\Phi^i = \begin{pmatrix} \Phi^i_{aa} & \Phi^i_{ab} \\ \Phi^i_{ba} & \Phi^i_{bb} \end{pmatrix} \tag{26}$$

Then equations (22) and (23) reduce to:

$$\hat{\boldsymbol{p}}^G_b = \left(\sum_{i=1}^{N} (\Phi^i_{bb})^{-1} \right)^{-1} \sum_{i=1}^{N} (\Phi^i_{bb})^{-1} \hat{\boldsymbol{p}}^i_b \tag{27}$$

$$\hat{\boldsymbol{p}}^{Gi}_a = \hat{\boldsymbol{p}}^i_a + \Phi^i_{ab} (\Phi^i_{bb})^{-1} (\hat{\boldsymbol{p}}^G_b - \hat{\boldsymbol{p}}^i_b) \tag{28}$$

Equations (27) and (28) give us a prescription to predict the outcome of the grand fit using only the results of the individual fits.

We now write S_G in terms of $\hat{\boldsymbol{p}}^G$, the solution to the grand fit as:

$$\begin{aligned} S_G &= S_{Go} + \sum_{i=1}^{N} (\boldsymbol{p}^i_a - \hat{\boldsymbol{p}}^{Gi}_a)^T M^i_{aa} (\boldsymbol{p}^i_a - \hat{\boldsymbol{p}}^{Gi}_a) \\ &\quad + 2(\boldsymbol{p}_b - \hat{\boldsymbol{p}}^G_b)^T \sum_{i=1}^{N} M^i_{ba} (\boldsymbol{p}^i_a - \hat{\boldsymbol{p}}^{Gi}_a) + (\boldsymbol{p}_b - \hat{\boldsymbol{p}}^G_b)^T \left(\sum_{i=1}^{N} M^i_{bb} \right) (\boldsymbol{p}_b - \hat{\boldsymbol{p}}^G_b) \qquad (29) \\ &= S_{Go} + (\boldsymbol{p} - \hat{\boldsymbol{p}}^G)^T M (\boldsymbol{p} - \hat{\boldsymbol{p}}^G) \qquad (30) \end{aligned}$$

where,

$$S_{Go} = \sum_{i=1}^{N} S_{io} + \sum_{i=1}^{N} (\hat{\boldsymbol{p}}^G_b - \hat{\boldsymbol{p}}^i_b)^T (\Phi^i_{bb})^{-1} (\hat{\boldsymbol{p}}^G_b - \hat{\boldsymbol{p}}^i_b) \tag{31}$$

$$\boldsymbol{p} = \begin{pmatrix} \boldsymbol{p}^1_a \\ \boldsymbol{p}^2_a \\ \boldsymbol{p}^3_a \\ \vdots \\ \boldsymbol{p}^N_a \\ \boldsymbol{p}_b \end{pmatrix} \quad , \quad M = \begin{pmatrix} M^1_{aa} & 0 & 0 & \cdots & 0 & M^1_{ab} \\ 0 & M^2_{aa} & 0 & \cdots & 0 & M^2_{ab} \\ 0 & 0 & M^3_{aa} & \cdots & 0 & M^3_{ab} \\ \vdots & \vdots & \vdots & \ddots & \vdots & \vdots \\ 0 & 0 & 0 & \cdots & M^N_{aa} & M^N_{ab} \\ M^1_{ba} & M^2_{ba} & M^3_{ba} & \cdots & M^N_{ba} & \sum_{i=1}^{N} M^i_{bb} \end{pmatrix} \tag{32}$$

The covariance matrix of the solution to the grand fit is give by $\Phi = M^{-1}$. The separate blocks of Φ can be expressed in terms of the single fit covariance matrices:

$$\Phi(\hat{\boldsymbol{p}}^{Gi}_a, \hat{\boldsymbol{p}}^{Gj}_a) = [\Phi^i_{aa} - \Phi^i_{ab} (\Phi^i_{bb})^{-1} \Phi^i_{ba}] \delta_{ij} + \Phi^i_{ab} (\Phi^i_{bb})^{-1} \left(\sum_{k=1}^{N} (\Phi^k_{bb})^{-1} \right)^{-1} (\Phi^j_{bb})^{-1} \Phi^j_{ba} \tag{33}$$

$$\Phi(\hat{\boldsymbol{p}}^{Gi}_a, \hat{\boldsymbol{p}}^G_b) = \Phi^i_{ab} (\Phi^i_{bb})^{-1} \left(\sum_{k=1}^{N} (\Phi^k_{bb})^{-1} \right)^{-1} \tag{34}$$

$$\Phi(\hat{\boldsymbol{p}}^G_b, \hat{\boldsymbol{p}}^G_b) = \left(\sum_{k=1}^{N} (\Phi^k_{bb})^{-1} \right)^{-1} \tag{35}$$

References

[1] Mazoyer BM, RH Huesman, TF Budinger, and BL Knittel. Dynamic PET data analysis. *J Comput Assist Tomogr*, **10**(4):645–653, 1986.

[2] Iida H, S Higano, N Tomura, F Shishido, I Kanno, S Miura, M Murakami, K Takahashi, H Sasaki, and K Uemura. Evaluation of regional differences of tracer appearance time in cerebral tissues using [^{15}O]water and dynamic positron emission tomography. *J Cereb Blood Flow Metab*, **8**:285–288, 1988.

[3] Huesman RH. A new fast algorithm for the evaluation of regions of interest and statistical uncertainty in computed tomography. *Phys Med Biol*, **29**(5):543–552, 1984.

[4] Budinger TF, Y Yano, SE Derenzo, RH Huesman, JL Cahoon, BR Moyer, WL Greenberg, and HA O'Brien, Jr. Myocardial uptake of rubidium-82 using positron emission tomography. *J Nucl Med*, **20**(6):603, 1979. (abstract).

[5] Budinger TF, SE Derenzo, RH Huesman, LG Sherman, BR Moyer, and Y Yano. Quantitative myocardial flow-extraction data using gated ECT. *J Nucl Med*, **21**(6):P16, 1980. (abstract).

[6] Budinger TF, Y Yano, BR Moyer, CH Mathis, E Ganz, RH Huesman, and SE Derenzo. Positron emission tomography of the heart. In Raynaud C, editor, *Nuclear Medicine and Biology: Proceedings of the Third World Congress of Nuclear Medicine and Biology; Paris, France, August 29 - September 2*, volume III, pages 2338–2341, Paris, 1982. Pergammon Press.

[7] Yano Y, TF Budinger, JL Cahoon, and RH Huesman. An automated microprocessor-controlled Rb-82 generator for positron emission tomography studies. In Knapp FF and TA Butler, editors, *Radionuclide Generators*, pages 97–122. American Chemical Society, Washington, DC, 1984.

[8] Huesman RH and BM Mazoyer. Kinetic data analysis with a noisy input function. *Phys Med Biol*, **32**(12):1569–1579, 1987.

[9] Phelps ME, SC Huang, EJ Hoffman, C Selin, L Sokoloff, and DE Kuhl. Tomographic measurement of local cerebral glucose metabolic rate in humans with (F-18)2-fluoro-2-deoxy-D-glucose: Validation of method. *Ann Neurol*, **6**:371–388, 1979.

[10] Friedland RP, TF Budinger, E Ganz, Y Yano, CA Mathis, B Koss, BA Ober, RH Huesman, and SE Derenzo. Regional cerebral metabolic alterations in dementia of the Alzheimer

type: Positron emission tomography with [^{18}F]fluoro-deoxyglucose. *J Comput Assist Tomogr*, **7**(4):590–598, 1983.

[11] Jagust WJ, TF Budinger, RH Huesman, RP Friedland, BM Mazoyer, and BL Knittel. Methodologic factors affecting PET measurements of cerebral glucose metabolism. *J Nucl Med*, **27**(8):1358–1361, 1986.

[12] Huesman RH and PG Coxson. Consolidation of common parameters in dynamic PET data analysis. In *Conference Record of the 1990 IEEE Nuclear Science Symposium, Arlington, VA*, volume 2, pages 1572–1576, 1990.

Table 1: Separate Fits for the Five Injections of Example 1

Study	$k_{21} \pm \sigma(k_{21})$	$k_{12} \pm \sigma(k_{12})$	$f_v \pm \sigma(f_v)$	$\rho(f_v, k_{21})$	$\rho(f_v, k_{12})$
1	0.855 ± 0.063	0.110 ± 0.046	0.204 ± 0.039	-0.01	-0.42
2	0.546 ± 0.038	0.012 ± 0.035	0.173 ± 0.032	-0.07	-0.40
3	0.459 ± 0.039	0.037 ± 0.044	0.163 ± 0.031	-0.18	-0.40
4	0.672 ± 0.046	0.032 ± 0.036	0.134 ± 0.034	-0.01	-0.37
5	0.670 ± 0.044	0.016 ± 0.034	0.163 ± 0.038	0.03	-0.41

Table 2: Grand Fit and its Approximation for the Five Injections of Example 1

	Grand Fit			Grand Taylor Fit		
Study	f_v	k_{21}	k_{12}	f_v	k_{21}	k_{12}
1	0.166	0.857	0.130	0.166	0.855	0.129
2		0.546	0.015		0.546	0.015
3		0.458	0.035		0.458	0.035
4		0.673	0.019		0.672	0.019
5		0.670	0.015		0.670	0.015

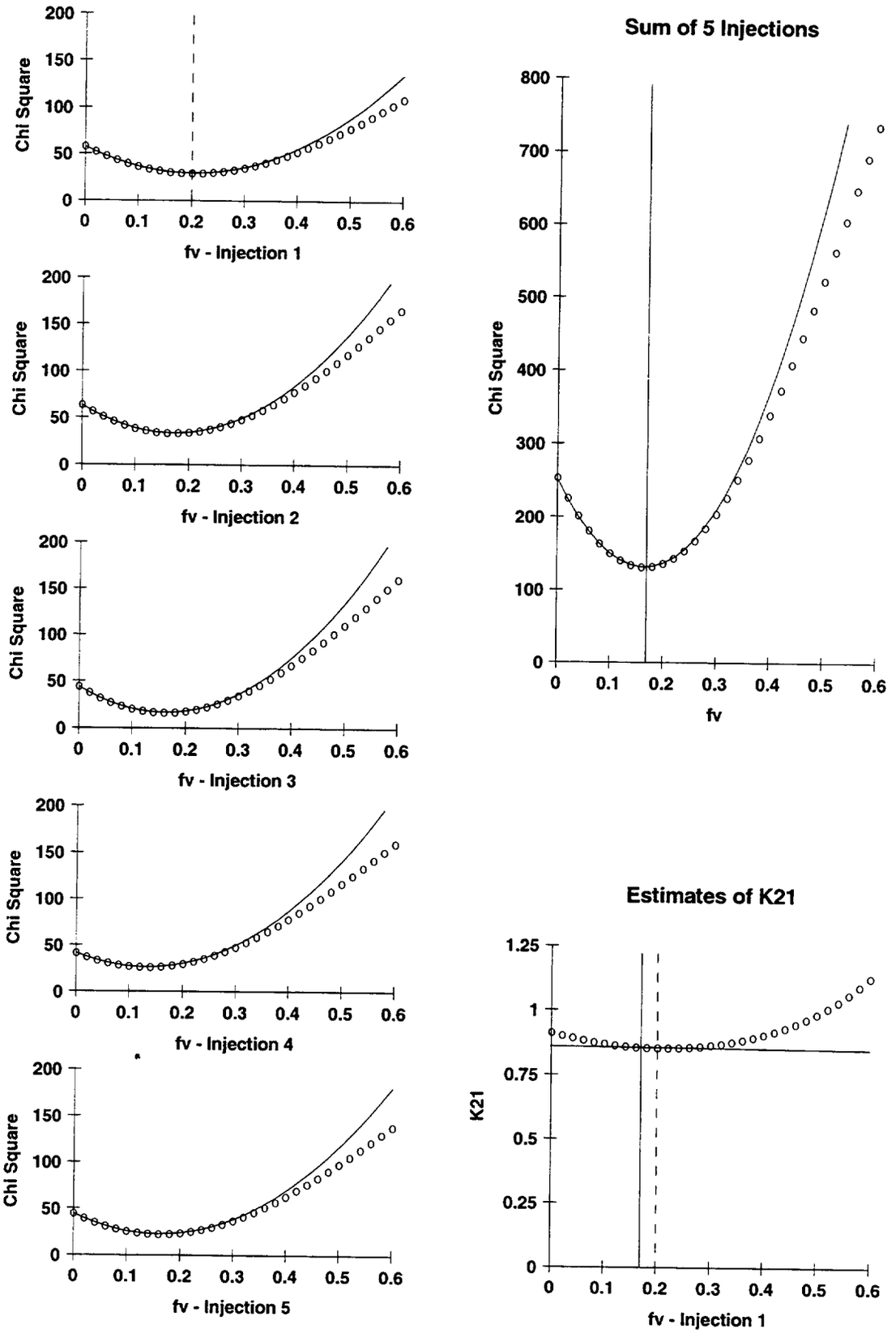

Figure 1: Plots of the Criteria for the Five Injections of Example 1

Table 3: Separate Fits for the Six Regions of Example 2

Region	$k_{21} \pm \sigma(k_{21})$	$k_{12} \pm \sigma(k_{12})$	$k_{32} \pm \sigma(k_{32})$	$f_v \pm \sigma(f_v)$	$t_0 \pm \sigma(t_0)$
1	0.126 ± 0.013	0.177 ± 0.042	0.084 ± 0.011	0.056 ± 0.013	-7.0 ± 1.5
2	0.112 ± 0.016	0.152 ± 0.056	0.094 ± 0.018	0.043 ± 0.015	-13.4 ± 1.3
3	0.131 ± 0.011	0.163 ± 0.031	0.073 ± 0.008	0.048 ± 0.014	-13.0 ± 1.1
4	0.114 ± 0.015	0.148 ± 0.048	0.085 ± 0.015	0.058 ± 0.015	-11.4 ± 1.1
5	0.225 ± 0.044	0.443 ± 0.143	0.098 ± 0.013	-0.029 ± 0.007	-16.5 ± 0.9
6	0.150 ± 0.017	0.183 ± 0.044	0.072 ± 0.010	0.037 ± 0.019	-13.7 ± 1.8

Region	$\rho(t_0, k_{21})$	$\rho(t_0, k_{12})$	$\rho(t_0, k_{32})$	$\rho(t_0, f_v)$
1	-0.17	-0.16	-0.03	0.41
2	-0.30	-0.26	-0.08	0.69
3	-0.30	-0.26	0.01	0.71
4	-0.19	-0.17	-0.04	0.43
5	0.28	0.26	0.12	-0.46
6	-0.35	-0.31	0.01	0.83

Table 4: Grand Fit and its Approximation for the Six Regions of Example 2

	Grand Fit					Grand Taylor Fit				
Region	t_0	k_{21}	k_{12}	k_{32}	f_v	t_0	k_{21}	k_{12}	k_{32}	f_v
1	-12.8	0.146	0.231	0.085	0.016	-13.1	0.135	0.204	0.085	0.034
2		0.110	0.146	0.093	0.047		0.110	0.149	0.094	0.045
3		0.130	0.162	0.073	0.049		0.131	0.164	0.073	0.046
4		0.119	0.163	0.086	0.046		0.118	0.160	0.086	0.049
5		0.232	0.468	0.101	-0.023		0.268	0.573	0.103	-0.041
6		0.147	0.177	0.072	0.044		0.148	0.179	0.072	0.042

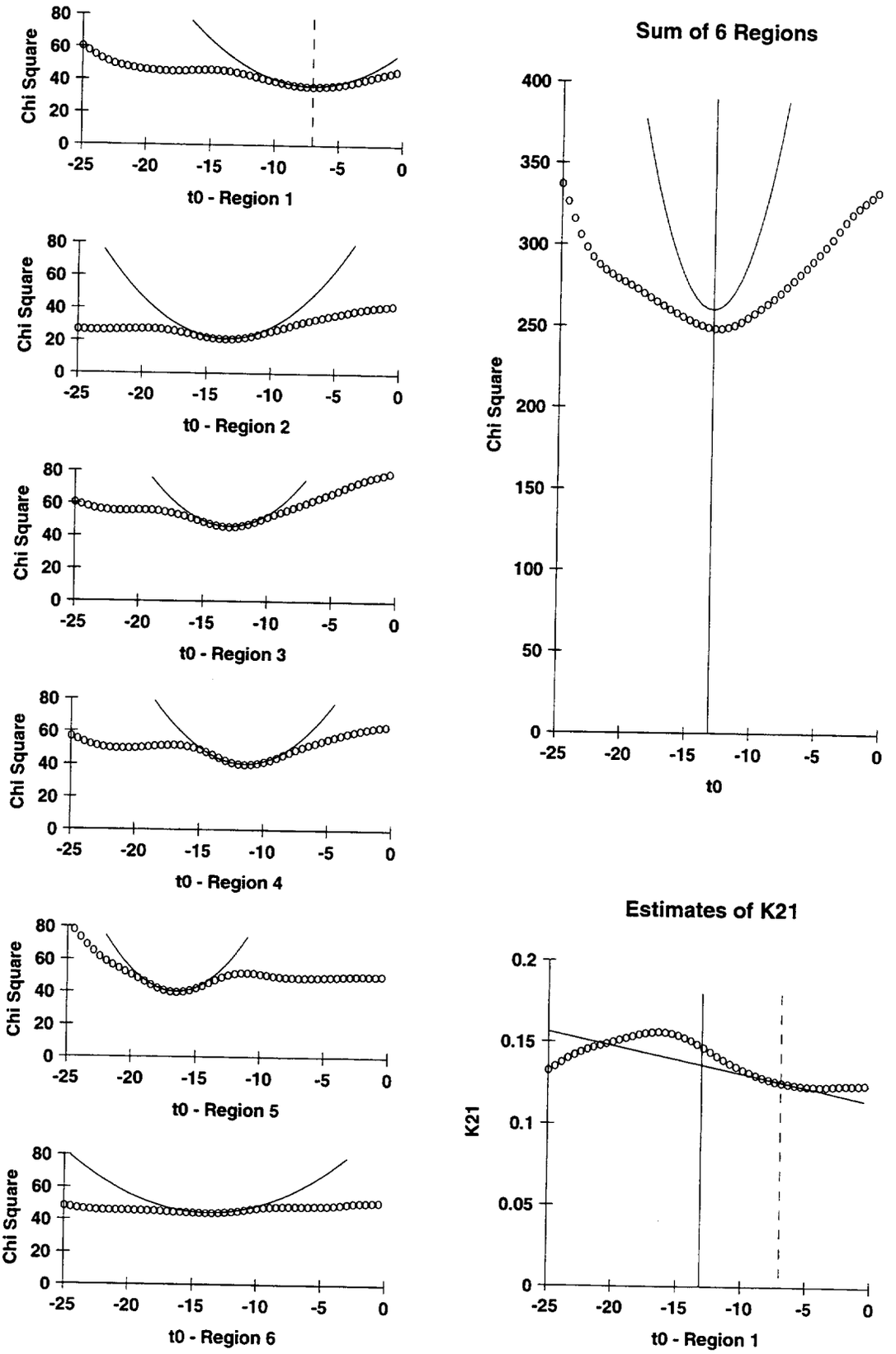

Figure 2: Plots of the Criteria for the Six Regions of Example 2